APPLIED PHYSICS LETTERS **97**, 031119 (2010)

Continuous wave laser generation at 1064 nm in femtosecond laser inscribed Nd:YVO$_4$ channel waveguides

Yang Tan,[1] Feng Chen,[1,2,a)] J. R. Vázquez de Aldana,[3] G. A. Torchia,[4] A. Benayas,[5] and D. Jaque[5]
[1]*School of Physics, Shandong University, Jinan 250100, People's Republic of China*
[2]*State Key Laboratory of Crystal Materials, Shandong University, Jinan 250100, People's Republic of China*
[3]*Grupo de Optica, Facultad de Ciencias, Universidad de Salamanca, Salamanca 37008, Spain*
[4]*Centro de Investigaciones Ópticas, CIC-Conicet, CC 124, La Plata 1900, Argentina*
[5]*Departamento de Física de Materiales, Facultad de Ciencias, Universidad Autónoma de Madrid, Madrid 28049, Spain*

(Received 29 April 2010; accepted 2 July 2010; published online 23 July 2010)

We report on continuous wave 1064 nm laser generation from an ultrafast laser inscribed neodymium-doped yttrium orthovanadate channel waveguide with pumping at 808 nm. Single-mode stable laser operations have been observed with pump powers at threshold as low as 14 mW and with laser slope efficiencies as high as 38.7%. *© 2010 American Institute of Physics*. [doi:10.1063/1.3467816]

Neodymium-doped yttrium orthovanadate (Nd:YVO$_4$) is one of most used gain media for solid state laser generation owing to its outstanding features (high emission cross section, broad absorption bands, good mechanical and thermal properties).[1,2] With respect to bulk lasers, waveguide lasers offer reduced active volumes and consequently much higher optical intracavity intensities, leading to low pumping thresholds and enhanced efficiencies.[3] This, in addition with their micrometric sizes, makes waveguide lasers one of the basic components of the modern integrated photonic systems.[4,5] In practice, the two-dimensional (2D) waveguides (i.e., in configurations of surface or buried channel/ridge) are more popular than the one-dimensional guiding structures owing to the stronger spatial confinement of light, reaching higher optical intensities within more compact scales.[4,5] Up to now, ion implantation and Nd ion indiffusion have been utilized to form waveguides in Nd:YVO$_4$ crystals.[6–9] Particularly, waveguide lasers at 1064 nm were realized for C ion-implanted Nd:YVO$_4$ channel waveguides.[10] Further improvement of the obtained laser performance are expected from a three-dimensional (3D) waveguide that optimizes light confinement and reduces propagation losses. Femtosecond (fs) laser writing has recently emerged as one of the most efficient techniques for direct 3D microfabrication of transparent optical materials.[11] Indeed it has been applied to fabricate buried channel waveguides in a number of optical materials, including optical crystals, ceramics, glasses, and polymers.[12–15] In addition, by using fs-laser inscription, single-mode waveguides could be easily obtained with relatively low propagation losses.[16] Very recently, we reported on the fabrication and characterization of Nd:YVO$_4$ channel waveguides produced by the direct fs-laser inscription.[17] The well-preserved photoluminescence features in the guiding structures suggested the potential applications of the formed channel waveguides as efficient integrated laser generation elements. In this paper, we report on the evidence of continuous wave (cw) laser actions from a fs-laser inscribed Nd:YVO$_4$ channel waveguide.

We used an amplified Ti:sapphire laser system (120 fs, 796 nm, and 1 kHz repetition rate) to write buried channel waveguides in the Nd:YVO$_4$ crystal (*a*-cut, doped by 1 at. % Nd^{3+} ions). The waveguide inscription parameters were as same as those used in Ref. 17 (i.e., 13 μJ/pulse and 50 μm/s of translation speed). Figure 1(a) shows the 2D refractive index profile of channel waveguides at the cross section. Based on this index distribution, we have calculated the modal profile of waveguides [Fig. 1(b)] by a so-called finite difference beam propagation method.[18] Compared with the measured near-field intensity distribution [Fig. 1(c)], one can conclude that there is a reasonable agreement between the calculated and experimental data. The propagation loss of the channel waveguides was found to be as low as $\sim$1 dB/cm.

The waveguide laser experiments were performed by using an end-face coupling system (see Fig. 2 for schematic of the setup). A cw Ti:sapphire laser (Coherent MBR 110) generated a polarized beam at 808 nm. A 20× microscope objective lens (N.A.=0.4) focused this pump light beam (polarized along *a*-axis of the crystal) into the channel waveguides. The generated laser beam at 1064 nm from the waveguide's output facet was collected by another 20× microscope objective and separated from the residual pump through a dichroic beam splitter. The spectrum of the trans-

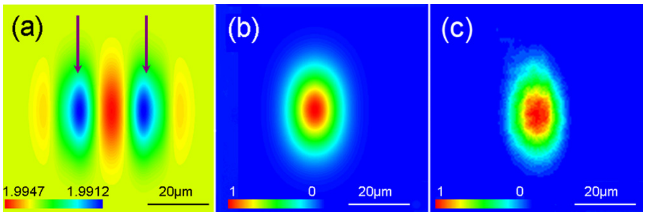

FIG. 1. (Color online) (a) Reconstructed 2D refractive index profile of the channel waveguide on the cross section, (b) calculated modal profile, and (c) measured near-field intensity distribution of waveguide mode. Arrows indicate the location of filaments.

[a)] Electronic mail: drfchen@sdu.edu.cn.

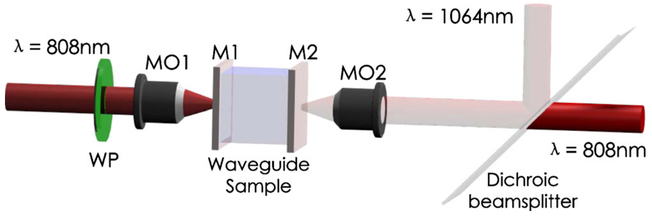

FIG. 2. (Color online) Schematic of the experimental setup for the waveguide laser generation. WP: wave plate; MO1 and MO2: microscope objective lens; M1 and M2: laser cavity mirrors adhered to the two end-facets of the sample.

mitted light was analyzed by a spectrometer. The laser gain experiments were performed either with or without cavity mirrors. In the former case, two mirrors [a mirror with transmission of 98% at 808 nm and reflectivity >99% at 1064 nm for the front face, and a mirror with reflectivity >99% at 808 nm and ~95% at 1064 nm as the output coupler (OC)] were adhered to the two end-facet with low fluorescence immersion oil, composing the laser cavity with OC efficiency of 5%. In the later case (without using any laser mirror), the laser generation has been realized by directly using the two polished facets (i.e., the air-crystal interface). The transmittance of the crystal's faces can be estimated from the refractive index of Nd:YVO_4 ($n \approx 2$) to be close to 90%.

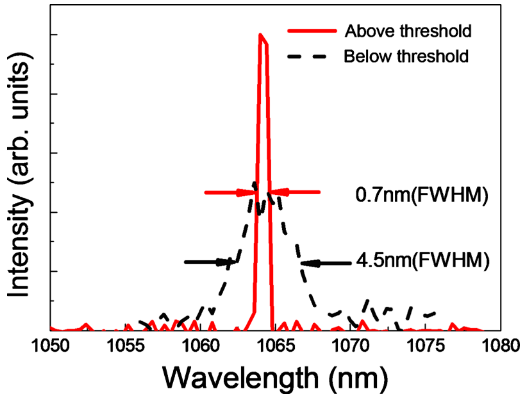

FIG. 3. (Color online) cw laser oscillation spectra (solid line) from the fs-laser inscribed Nd:YVO_4 waveguide after pumping at 808 nm above the pumping threshold. The luminescence emission spectra of the waveguides (when the pumping power is below the threshold) are also shown for comparison (dashed line).

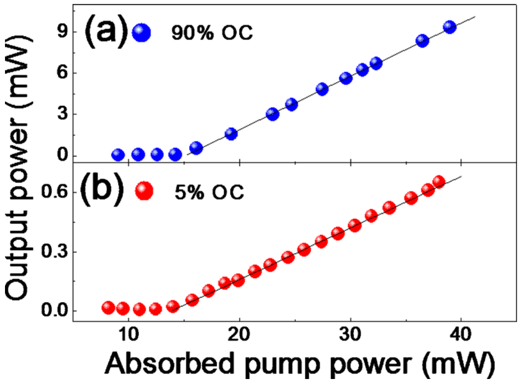

FIG. 4. (Color online) cw waveguide laser output power at 1064 nm as a function of the absorbed pump power at 808 nm (a) without or (b) with the mirrors. The slope efficiency of 38.7% and 0.6%, and the threshold of ~15 and 14 mW can be obtained for laser generations from the Nd:YVO_4 channel waveguides without or with the cavity mirrors, respectively.

Figure 3 shows the emission spectra around 1064 nm from the Nd:YVO_4 channel waveguide at two different absorbed pump powers (~14 and ~28 mW) obtained without using any cavity mirrors. As one can see, the full width at half maximum (FWHM) of the emission line is ~4.5 nm when absorbed pump power is 14 mW, while becomes narrower when the absorbed pump power is increased up to ~28 mW. For such absorbed pump powers, the FWHM emission line was 0.7 nm centered at 1064 nm (where the emission cross section of Nd:YVO_4 peaks), denoting the presence of laser oscillation. This is further confirmed by the laser gain curves of Fig. 4(a), in which the output power (at 1064 nm) generated in the Nd:YVO_4 waveguide as a function of the absorbed pump power (at 808 nm). From the linear fit (solid line) of the experimental data (dots) we can determine a laser threshold (P_{th}) of 15 mW and a laser slope efficiency (Φ) of 38.7% [Fig. 4(a)]. The maximum 1064 nm laser power achieved was 9.5 mW for the maximum absorbed pump power of 39 mW, leading to an optical conversion efficiency of 24% (9.5 mW/39 mW). It may be noted that the laser performance depicted in Fig. 4(a) constitutes a relevant improvement with respect to that previously reported from Nd:YVO_4 channel waveguides fabricated by carbon implantation. In such waveguides the laser threshold was ~45 mW and the Φ was 29%.[10] The P_{th} and Φ in this four level system can be expressed as[19]

$$P_{th} = \frac{hc}{\lambda_p}\frac{1}{\eta\sigma_e\tau}\frac{\delta}{2}A_{eff}, \tag{1}$$

$$\Phi = \eta\frac{(T_1+T_2)}{\delta}\frac{\lambda_P}{\lambda_L}, \tag{2}$$

where h is the Planck's constant, c is the light velocity in the vacuum, λ_L and λ_P are the wavelengths of the laser and pump beams, respectively, σ_e is the stimulated emission cross section (1.2×10^{-18} cm^2), τ is the fluorescence lifetime (90 μs), A_{eff} is the effective pump area (600 μm^2), η is the fraction of absorbed photons that contribute to the population of the $^4F_{3/2}$ metastable state ($\eta \approx 1$), and $T_1 = T_2 = 0.9$ are the transmittance of the end-faces, δ is the round-trip cavity loss exponential factor and could be expressed by the propagation loss (α) and the transmittance of end-facets

$$\delta = 2\alpha L - \ln[(1-T_1)\times(1-T_2)]. \tag{3}$$

The loss α of the fs-laser inscribed waveguide (~1 dB/cm) is much lower than that of the implanted waveguide (~8 dB/cm), resulting an obvious reduction in δ, which may be one important reason for the improved behaviors in P_{th} and Φ.

Based on Eqs. (1) and (2), a relationship between P_{th} and Φ could be found and expressed as the following equation:

$$P_{th}\Phi = \frac{hc(T_1+T_2)}{2\lambda_L\sigma_e\tau}A_{eff}. \tag{4}$$

According to Eq. (4) and the measured slope efficiency, a laser threshold of 10 mW has been calculated,[20] which is in reasonable agreement with the value found experimentally (15 mW).

In the case of 5% OC coefficient, P_{th} has been decreased to be ~14 mW and Φ is only ~0.6% [Fig. 4(b)]. The decrease in Φ when decreasing the OC transmittance was indeed predicted by Eq. (2) since it decreases the optical extraction efficiency. In addition, the optical losses associated to the crystal-immersion oil-OC interface could be also contributing to the measured reduction in the slope efficiency.

In summary, we have reported the stable 1064-nm laser oscillations at room temperature from a $\mathrm{Nd:YVO_4}$ channel waveguides fabricated by fs laser inscription. Owing to the low propagation losses, the threshold has been found to be as low as ~14 mW with laser slope efficiency of 38.7%. The maximum output light power is about ~9.5 mW at 1064 nm. The good laser performance suggests potential applications on construction of integrated laser devices in $\mathrm{Nd:YVO_4}$.

This work was supported by National Natural Science Foundation of China (Grant No. 10925524), the Spanish Ministerio de Ciencia y Tecnología (Grant Nos. MAT2007-64686, MAT2009-06580-E/MAT, CSD2007-00013, and FIS2009-09522), UAM and Comunidad Autonoma de Madrid (Grant Nos. CCG08-UAM/MAT-4434 and PHAMA P2009/MAT1756) and CONICET (Grant No. PIP 11220090100394).

[1] A. A. Kaminskii, *Laser Crystals: Their Physics and Properties* (Springer, New York, 1990).
[2] T. Taira, A. Mukai, Y. Nozawa, and T. Kobayashi, Opt. Lett. **16**, 1955 (1991).
[3] J. I. Mackenzie, IEEE J. Sel. Top. Quantum Electron. **13**, 626 (2007).
[4] S. E. Miller, Bell Syst. Tech. J. **48**, 2059 (1969).
[5] G. Lifante, *Integrated Photonics: Fundamentals* (Wiley, New York, 2008).
[6] G. Vázquez, M. Sánchez-Morales, H. Márquez, J. Rickards, and R. Trejo-Luna, Opt. Commun. **240**, 351 (2004).
[7] F. Chen, X. L. Wang, K. M. Wang, Q. M. Lu, and D. Y. Shen, Appl. Phys. Lett. **80**, 3473 (2002).
[8] F. Chen, L. Wang, Y. Jiang, X. L. Wang, K. M. Wang, G. Fu, Q. M. Lu, C. E. Ruter, and D. Kip, Appl. Phys. Lett. **88**, 071123 (2006).
[9] S. J. Hettrick, J. S. Wilkinson, and D. P. Shepherd, J. Opt. Soc. Am. B **19**, 33 (2002).
[10] M. Sánchez-Morales, G. Vázquez, E. Mejía, H. Márquez, J. Rickards, and R. Trejo-Luna, Appl. Phys. B: Lasers Opt. **94**, 215 (2009).
[11] S. Juodkazis, V. Mizeikis, and H. Misawa, J. Appl. Phys. **106**, 051101 (2009).
[12] M. Ams, G. D. Marshall, P. Dekker, J. A. Piper, and M. J. Withford, Laser Photonics Rev. **3**, 535 (2009).
[13] G. A. Torchia, A. Rodenas, A. Benayas, E. Cantelar, L. Roso, and D. Jaque, Appl. Phys. Lett. **92**, 111103 (2008).
[14] P. Nandi, G. Jose, C. Jayakrishnan, S. Debbarma, K. Chalapathi, K. Alti, A. K. Dharmadhikari, J. A. Dharmadhikari, and D. Mathur, Opt. Express **14**, 12145 (2006).
[15] W. Watanabe, S. Sowa, and K. Itoh, Proc. SPIE **6108**, 61080R (2006).
[16] S. Nolte, M. Will, J. Burghoff, and A. Tuennermann, Appl. Phys. A: Mater. Sci. Process. **77**, 109 (2003).
[17] W. F. Silva, C. Jacinto, A. Benayas, J. R. Vazquez de Aldana, G. A. Torchia, F. Chen, Y. Tan, and D. Jaque, Opt. Lett. **35**, 916 (2010).
[18] Rsoft Design Group, Computer software BEAMPROP, (http://www.rsoftdesign.com).
[19] E. Lallier, J. P. Pocholle, M. Papuchon, M. P. De Micheli, M. J. Li, Q. He, D. B. Ostrowsky, C. Grezes-Besset, and E. Pelletier, IEEE J. Quantum Electron. **27**, 618 (1991).
[20] L. Fornasiero, S. Kück, T. Jensen, G. Huber, and B. H. T. Chai, Appl. Phys. B: Lasers Opt. **67**, 549 (1998).